Electroactive 3D printable poly (3,4-ethylenedioxythiophene)-*graft*-poly(ε-caprolactone) copolymers as scaffolds for muscle cell alignment

Antonio Dominguez-Alfaro,[a,b] Miryam Criado-Gonzalez,[a] Elena Gabirondo,[a] Haizpea Lasa-Fernández,[b] Jorge L. Olmedo-Martínez,[a] Nerea Casado,[a] Nuria Alegret,[b,c] Alejandro J. Müller,[a,e] Haritz Sardon,[a] Ainara Vallejo-Illarramendi[c,d] and David Mecerreyes*[a,e]

The development of tailor-made polymers to build artificial three-dimensional scaffolds to repair damaged skin tissues is gaining increasing attention in the bioelectronics field. Poly (3,4-ethylene dioxythiophene) (PEDOT) is the gold standard conducting polymer for the bioelectronics field due to its high conductivity, thermal stability, and biocompatibility; however, it is insoluble and infusible, which limits its processability into three dimensional scaffolds. Here, poly(3,4-ethylendioxythiophene)-*graft*-poly(ε–caprolactone) copolymers, PEDOT-*g*-PCL, with different molecular weights and PEDOT compositions, were synthesized by chemical oxidative polymerization to enhance the processability of PEDOT. First, the chemical structure and composition of the copolymers were characterized by nuclear magnetic resonance, infrared spectroscopy, and thermogravimetric analysis. Then, the additive manufacturing of PEDOT-*g*-PCL copolymers by direct ink writing was evaluated by rheology and 3D printing assays. The morphology of the printed patterns was further characterized by scanning electron microscopy and the conductivity by the four-point probe. Finally, the employment of these printed patterns to induce muscle cells alignment was tested, proving the ability of PEDOT-*g*-PCL patterns to produce myotubes differentiation.

Introduction

Conducting polymers (CPs) with tunable electrical and mechanical functionalities are gaining increasing attention for the development of (bio)electronic devices such as electronic skin, biosensors, health monitoring electrodes or soft robotics.[1-3] The additive manufacturing (AM) of CPs also plays a key role in the final properties of these electroactive objects, which makes it necessary to evolve from traditional two-dimensional (2D) thin films to shape-conformable three-dimensional (3D) structures.[4-5] Besides, in muscle engineering applications, AM could improve interface cell-material throughout the manufacturing of artificial patterned scaffolds that support unidirectional alignment of myotubes forming parallel arrays of muscle, mimicking real scenarios.[6-7] In this regard, 3D printing of CPs has emerged in the last years as a versatile technique for the fabrication of electronic devices with structural defined shapes and functionalities at the micrometer scale.[8] Therefore, the design of tailor-made conducting polymer materials that possess good conductivity and appropriate mechanical properties to be processed by 3D printing represents a fascinating approach.[9-10]

Poly (3,4-ethylene dioxythiophene) (PEDOT) is one of the most used conducting polymers in the (bio)electronics field due to its commercial availability and inherent properties, *i.e.*, high conductivity, thermal stability, and biocompatibility; however, it is insoluble and infusible, which limits its processability.[11] This drawback can be overcome by stabilizing PEDOT with other polymers that provide the required properties to be processed by 3D printing techniques. PEDOT is usually stabilized with polystyrene sulfonate (PSS), leading to PEDOT:PSS dispersions that can be formulated with organic solvents or polymers, *i.e.*, cellulose, alginate, gelatin, leading to viscous materials (10^2 – 10^3 Pa·s) with shear-thinning properties to be processed by direct ink writing (DIW).[12-15]

Although simple blending is the easiest method to prepare processable PEDOT/polymer materials, miscibility issues can affect the structural and functional homogeneity of the manufactured material, which is undesirable and can be solved by covalent grafting of both homopolymers. This PEDOT functionalization depends on the molecular weight, functional groups, conformation, and side chains attached to the monomeric units to graft leading to copolymers that keep intact the conjugated PEDOT backbone, responsible of the conductive properties, while modulating the polymer physicochemical properties improving its processability.

Among different polymer materials that can be combined with PEDOT to synthesize processable and biocompatible copolymers, saturated polyesters such as polycaprolactone (PCL) or polylactide (PLA) are excellent candidates due to their biodegradability and biocompatibility.[16-17] Very recently, we have shown that PEDOT-*g*-PLA copolymers can be processed by 3D direct ink writing leading to scaffolds for soft tissue engineering.[18] Nevertheless, for hard tissue engineering applications, *i.e.*, skeletal muscle tissues, materials with longer degradation times are searched, being PCL an excellent alternative.[19] Moreover, PCL exhibits lower glass transition (T_g ≥ -60°C) and melting (T_m > 60°C) temperatures, and higher crystallization rate and flexibility than PLA,[20-21] which favours the additive manufacturing by DIW. In this line, Stevens and co-workers synthesized PEDOT-*co*-PCL block copolymers by ring opening polymerization of ε-caprolactone with oligo-EDOT macromonomers functionalized with amino end-caped groups to fabricate fiber-made platforms through melt electrospinning writing for neural tissue engineering.[22] Similar strategy was used to synthesize tetraaniline-*b*-PCL-*b*-tetraaniline copolymers to manufacture scaffolds for bone tissue engineering by DIW,[23] and PPy-

b-PCL scaffolds by electrohydrodynamic printing (EHD) for peripheral nerve injury repair.[24] Apart from that, EDOT end-group functionalized PCL macromonomers, synthesized by ROP of hydrozymethyl-EDOT and Ɛ-caprolactone in presence of Sn(Oct) catalyst, has shown their ability to self-assemble in selective organic solvents due to their hydrophobic amphiphile nature.[25]
In this work, we propose new PEDOT-*g*-PCL graft copolymers to manufacture electroactive scaffolds for muscle tissue engineering by DIW. These copolymers were synthesized through chemical oxidative polymerization of EDOT and new PCL macromonomers functionalized with an EDOT end group. The influence of the EDOT-PCL macromonomer molecular weight (M_n) on the copolymerization process, and its effect on the copolymer processability by extrusion printing and conductive properties were also evaluated. Finally, the biocompatibility of the PEDOT-*g*-PCL printed patterns was tested in contact with 8220 muscle cells, as well as their influence in the myoblast cell alignment for potential muscle tissue engineering applications.

Experimental section

Materials

Ɛ-Caprolactone (97%) was supplied by Sigma-Aldrich and distilled before using it. Methanesulfonic acid (MSA), 4-dimethylaminopyridine (DMAP), 3,4-Ethylenedioxythiophene (97%) (EDOT) and hydroxymethyl EDOT (95%) were provided by Sigma-Aldrich and used as received.

Synthesis of PCL macromonomers. Three different macromonomers with molecular weights comprise between 4 000 and 16 000 g mol^{-1}, PCL_{4k}, PCL_{8k} and PCL_{16k}, were synthesized by ring-opening polymerization (ROP) of ε-caprolactone in bulk using EDOT-methanol as chain initiator and an organocatalyst, formed by a mixture of methanesulfonic acid and 4-dimethylaminopyridine (1MSA:1DMAP). First, the organocatalysts mixture was warmed up at 100°C until forming a white salt. Then, the caprolactone and hydroxymethyl EDOT were added and allowed them to react at 130 °C with magnetic stirring and sealed under inert atmosphere for 5 days until 90% conversion is achieved. The resulting product, EDOT-PCL, was purified through precipitation in methanol, and subsequently vacuum-dried at room temperature overnight.

Synthesis of PEDOT-*g*-PCL copolymers. Graft copolymers with different compositions were obtained through chemical oxidative copolymerization of EDOT and PCL macromonomers using $FeCl_3$ as oxidizing agent and $CHCl_3$ as solvent. In a typical copolymer composition of 95%wt PCL and 5%wt PEDOT (95 PCL: 5 PEDOT), the PCL macromonomers synthesized previously (1.5 g, 1.31×10^{-2} mol) and EDOT (0.078 g, 5.49×10^{-4} mol) were dissolved in 10 mL of $CHCl_3$. Then, 0.135g of $FeCl_3$ (1.5eq respect EDOT monomer) was added to the mixture and let it react under magnetic stirring at room temperature overnight. The blue dispersion obtained was precipitated and washed with methanol until the iron residue was fully removed. Finally, the product was dried under vacuum at room temperature.

Methods

Nuclear magnetic resonance spectroscopy (NMR). ^{1}H-NMR was used to determine the conversion and the final composition of the copolymer, and ^{13}C-NMR was used to determine the tacticity. ^{1}H-NMR and ^{13}C-NMR spectra were recorded with a Bruker Advance DPX 300 at 300.16 and 75.5 MHz resonance frequency, respectively, at room temperature and using $CDCl_3$ as solvent. The experimental conditions for ^{1}H-NMR spectroscopy were: 10 mg of sample, 3 s acquisition time, 1 s delay time, 8.5 µs pulse, spectral width 5 000 Hz, and 32 scans. For ^{13}C-NMR spectroscopy: 39 mg of sample, 3 s acquisition time, 4 s delay time, 5.5 µs pulse, spectral width 18800 Hz, and more than 10000 scans.

Size Exclusion Chromatography / Static Light Scattering (SEC/MALLS). SEC/MALS measurements were carried out at 30°C on an Agilent 1200 system equipped with PLgel 5 µm Guard and PLgel 5 µm MIXED-C columns, a differential refractive index (RI) detector (Optilab Rex, Wyatt), and a SLS detector (Minidawn Treos, Wyatt). The SEC setup consisted of a pump (LC-20A, Shimadzu), an autosampler (Waters 717), a differential refractometer (Waters 2410), and three columns in series (Styragel HR2, HR4 and HR6 with pore sizes ranging from 102 to 106 Å). THF was used as eluent at a flow rate of 1 mL $min^{-1,}$ and values in THF were determined using an Optilab Rex Detector. The samples were diluted in THF, up to a concentration of 5 mg mL^{-1}, and filtered with a nylon filter (0.45 µm). Chromatograms were obtained in THF at 30 °C using a flow rate of 1 mL min^{-1}. The equipment was calibrated using narrow polystyrene standards ranging from 595 to 3.95×10^6 g mol^{-1} (5^{th} order universal calibration). Data analysis was performed with the Software ASTRA from Wyatt.

Matrix Assisted Laser Desorption Ionization-Time of Flight Mass Spectrometry (MALDI-TOF MS). The analysis was performed on an Ultraflextreme III time-of-flight mass spectrometer equipped with a pulsed Nd:YAG laser (355 nm). A mixture of trans-2-[3-(4-tert-Butylphenyl)-2-methyl-2-propenylidene]malonitrile (DCTB) and Silver trifluoroacetate matrix was used to acquire the spectra. The DCTB matrix was dissolved in THF at a concentration of 20 mg mL^{-1} and 1 mg mL^{-1} Silver trifluoroacetate (AgTFA) was added as cationic ionization agent. Then, the polymer sample is dissolved in THF at a concentration of 1 mg mL^{-1}, and mixed with the matrix at a ratio of 10:2:1 (matrix: sample: salt). A total of 2000 – 3000 acquisitions were carried out in positive linear mode and registered by the software FlexControl 3.3 (Bruker Daltonics, Bremen, Germany).

Fourier transform Infrared spectroscopy (FT-IR). Measurements were performed in a Thermo scientific Nicolet 6700 FT-IR spectrometer at room temperature. 2.5 mg sample was mixed with 1 g of KBr in a mortar. Then, the mixture was compressed,

forming a pill that was measured by solid-state IR spectroscopy. Spectra were recorded between 600 and 2200 cm^{-1} in transmission mode and applying 10 scans.

UV-Vis-NIR spectroscopy. Spectra were recorded with a Perkin-Elmer UV/Vis/NIR Lambda 950 spectrometer between 300 and 1000 nm using a quartz cuvette. 0.5 mg sample was diluted in 10 mL $CHCl_3$, and sonicated during 15 minutes.

Thermogravimetric analysis (TGA). Measurements were performed using a TGA Discovery (TA Instruments) under nitrogen atmosphere (flow rate of 25 mL min^{-1}). After a first equilibration step at 100°C for 20 min, the sample was heated from 100°C to 800°C at a rate of 10°C min^{-1}.

Atomic force microscopy (AFM). Surface topologies of copolymers were characterized by AFM (JPK NanoWizard II) in tapping mode in the conventional height mode at a nominal force constant of 42 N/m and 320 kHz resonant frequency. Nanoscope Analysis software was employed for the visualization and analysis of the AFM images. PEDOT-*g*-PCL copolymers and macromonomer were dissolved in chloroform at room temperature at 0.1 wt%. Then, samples were spin-coated on a previously cleaned Si wafer (1 cm^2), forming thin films with 20 nm thickness. For the pre-thermal treatment, the samples were dried at room temperature while with post-treatment the samples were warmed up at 20°C min^{-1} until T_m and cooled down at the same scan rate until room temperature.

Differential scanning calorimetry (DSC). A Perkin Elmer DSC 8000 equipment was used to carry out the DSC experiments. The sample mass was kept constant at approximately 5 mg, and aluminium pans were used. DSC experiments were carried out in between −20 and +120 °C, and the cooling and heating scans were recorded at 20 °C min^{-1}.

Scanning electron microscopy (SEM). SEM measurements were performed on a JEOL JSM-6490LV microscope at 3-5kV, and running in a point by point scanning mode. In the case of films, cylindrical glass coverslip (11 mm diameter) were previously cleaned with isopropanol, by sonication for 15 min, in order to remove impurities, and dried at room temperature. Then, 25 mg sample was solubilized in 1 mL of chloroform, sonicated for 15 minutes and drop-casted on the coverslip. Then, the films were dried at room temperature to remove the solvent. In the case of the printed scaffolds, they were directly observed after printing without further treatment.

Rheological measurements. Rheological tests were performed using an ARES rheometer (Rheometrics) at the melting temperature of the copolymers or macromonomers, 65 °C. Parallel aluminum plates of 25 mm diameter were employed. Frequency sweeps were carried out from 0.1 to 100 Hz at a constant strain of 1%.

3D Printing. The printing process was carried out using a 3D-Bioplotter (Developer Series, EnvisionTEC, Gladbeck, Germany), and the printed geometries were designed with the software Autodesk Inventor 2019. The printing process was performed at 65 °C, a maximum pressure of 4×10^5 Pa and 0.001 mm of maximum resolution. Needles with an inner diameter of 0.3 mm were used. Scaffolds used for the morphological and electrical characterization were printed over a Teflon sheet. In contrast, PCL and PEDOT-*g*-PCL patterns used for biological tests were printed in two steps: (*i*) a first solid copolymer layer were printed and then (*ii*) zig-zag patterns were printed on top.

Contact angle. The surface wettability was determined by static contact angle measurements, through the sessile drop method, using a standard OCA 20 goniometer (Dataphysics) and recorded with the SCA 20 software under ambient conditions. A water droplet of 3 µL was deposited on the PCL and PEDOT-*g*-PCL printed patterns and contact angle was measured within five seconds. The analysis of contact angles from recorded pictures was also made with the SCA 20 software. Three different samples were measured and results were shown as mean ± standard deviation.

Conductivity. The conductivity was measured on a four-point probe Ossila Sheet using more than three different zones of the film. Samples were prepared by drop casting 100 µL of each dispersion (1 mg mL^{-1} in $CHCl_3$) on glass coverslips, and dried at room temperature to remove the solvent leading to dry sheets. Previously to measure the conductivity, the thickness of the sheets was measured with a digital caliper. Then, the electrical conductivity was calculated, taking into account the thickness of the sample.

Electrochemical Characterization. Cyclic voltammetry was performed using a VMP-3 potentiostat (Biologic Science Instruments) in a three-electrode setup, employing a platinum wire as counter electrode, Ag/AgCl as the reference electrode and glassy carbon as working electrode. PEDOT-*g*-PCL and PCL were dissolved in chloroform (34 mg mL^{-1}) and drop-casted (15 µL) into a glassy carbon electrode. The obtained electrodes were dried at room temperature for 1 hour before the measurement. 0.1 M NaCl aqueous solution was used as electrolyte, which was purged with nitrogen for 15 min before the experiment. Cyclic voltammetry was carried out in the potential range of −0.2 to 0.8 V vs. Ag/AgCl at 50 mV s^{-1} and at 50, 100, 150, 200 and 250 mV s^{-1} for the scan rate experiment.

***In vitro* cell culture of Immortalized human myoblasts.** The immortalized human myoblast cell line 8220 was provided by Dr. Vincent Mouly and generated on the Platform for the Immortalization of Human Cells, at the Myology Institute in Paris (France). Cells were incubated at 37 °C in a saturated humidity atmosphere containing 95% air and 5% CO_2. At confluence, cells were trypsinized and seeded on the 3D printed patterns at a density of 125×10^5 cells per sample. Gelatin-coated plates (0.5% gelatin) were used as controls. The proliferation medium consisted of Promocell Skeletal Growth Medium (SGM) supplemented with 10% FBS, 1% Glutamax, and 1% gentamicin (both from Gibco-Invitrogen). Once the cells reached 100% confluency, the proliferation medium was replaced by a basic differentiation medium containing: DMEM 10 µg mL^{-1} insulin, 100 µg mL^{-1} apotransferrin, and 50 µg mL^{-1} gentamicin.

Lactate dehydrogenase (LHD) assay. For the cytotoxicity assay, 5 000 cells were seeded in each 96-plate well (n=8 wells per condition). After 24 hours, supernatants were collected, and the amount of lactate dehydrogenase (LDH) was measured using

Cytotox 96 kit (Promega). Briefly, 50 µL of cell supernatants were incubated with reaction solution for 30 min at room temperature in the dark. Then, the reaction was stopped and absorbance or optical density (OD) was measured at 492 nm. The absorbance was normalised to the signal obtained in control wells for the graph representation.

SEM Imaging of the Cell Morphology on the scaffolds. After cell culture, samples were firstly dehydrated with a gradient of ethanol solutions (60%, 70%, 80%, 90%, and 100% v/v ethanol in Milli-Q water) for 1 h each at room temperature. Then, a second dehydration process was carried out with hexamethyldisilazane (HMDS) in ethanol gradient solutions (30%, 50%, 70%, 90%, and 100%) for 30 min each step. Finally, samples were air-dried, sputter-coated with gold (Alto 1000, Gatan Inc.), and visualized by SEM operated in secondary electron detection mode.

Immunofluorescence. First, cells were fixed with 4% paraformaldehyde (PFA) in phosphate buffer saline (PBS) for 15 min at room temperature. Then, they were permeabilized and blocked with 0.5% Triton X-100 and 2% BSA in PBS for 1 hour. They were incubated with FITC-conjugated Myosin Heavy Chain-CFS monoclonal antibody (R&D Systems) for 1h at a dilution 1:50 in PBS at room-temperature. Then, samples were washed with PBS three times, and they were mounted with ProLong Gold antifade reagent with DAPI (Life Technologies). Fluorescence images were acquired using a Zeiss LSM 510 confocal microscope with a 20X objective.

Table 1. Chemical oxidative copolymerization of EDOT with PCL macromonomers of different M_n in $CHCl_3$ at room temperature overnight.

code	$M_{n\ PCL}$ (g mol^{-1})[a]	%wt $_{EDOT}$[b]	Yield (wt%)	%wt $_{PEDOT}$[c]
1	4 000	10	12	40
2	7 500	5	40	16
3	7 500	10	26	26
4	7 500	20	18	68
5	16 000	5	50	10
6	16 000	10	35	30

[a] M_n EDOT-PCL macromonomers calculated by ^{1}H-NMR. [b] Weight fraction of EDOT in the reaction feed. [c] Weight fraction of PEDOT in the copolymers calculated by TGA.

Results and discussion

Synthesis of α–EDOT-PCL macromonomers by ring-opening polymerization

Graft copolymers combining conducting polymers, *i.e.*, PEDOT or polypyrrole, and aliphatic polyesters have been successfully synthesized by the macromonomer method.[18, 26-29] However, to the best of our knowledge, the graft copolymerization of PEDOT and PCL using α–EDOT-PCL macromonomers has not been reported yet. For such purpose, in a first step α–EDOT-PCL macromonomers, with molecular weights ranging from 4000 to 16000 g mol^{-1}, were synthesized by ring-opening polymerization (ROP) using EDOT-methanol as chain initiator of ε-caprolactone polymerization (**Scheme 1a**). The ROP was carried out in bulk using an organocatalyst previously reported for the synthesis poly(L-lactide) (PLA) using benzyl alcohol as initiator. This organocatalyst is formed by a mixture of methanesulfonic acid (MSA) and 4-dimethylaminopyridine (DMAP) in a ratio 1:1.[30] A 90% conversion was reached after 5 days reaction at 130°C as calculated by ^{1}H-NMR (**Figure S1a**, Supporting Information). Moreover, the molecular weight of the EDOT-PCL macromonomers was determined through the relative intensities of the ^{1}H-NMR signals corresponding to the tiophene proton at 6.4 ppm and -CH_2- aliphatic polyester chain at 4.3 ppm (**Table S1**, Supporting Information). The presence of the EDOT end group was also confirmed by ^{13}C-NMR (**Figure S1b**, Supporting Information). Matrix-assisted laser desorption ionization-time of flight (MALDI-TOF) spectroscopy (**Figure S1c**, Supporting Information) also confirmed the presence of the end-group and a monomodal mass profile distribution of the polycaprolactone repeating unit (114 m/z).

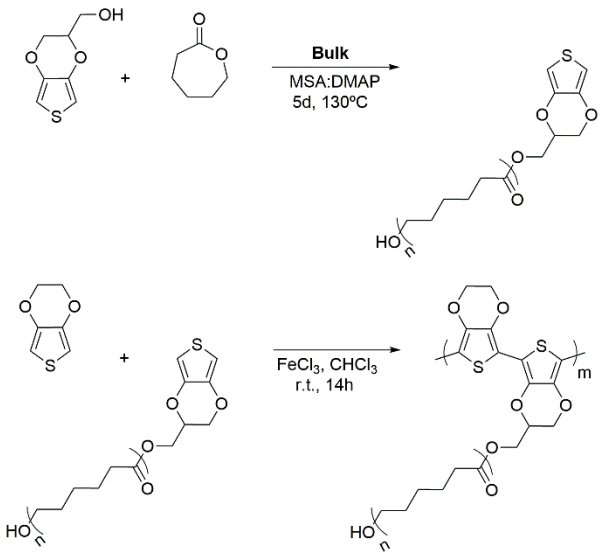

Scheme 1. Chemical routes employed to synthesize: a) EDOT-PCL macromonomers by ROP and b) PEDOT-*g*-PCL copolymers by chemical oxidative polymerization.

Synthesis and characterization of PEDOT-*g*-PCL copolymers

PEDOT-*g*-PCL copolymers were synthesized by chemical oxidative copolymerization of 3,4-ethylendioxythiophene and the previously synthesized PCL macromonomers (**Scheme 1b**). Thus, the EDOT monomer was oxidized with an excess of $FeCl_3$ and grafted to the EDOT-PCL macromonomer in solution leading to a dark blue dispersion. It is expected that the conductive properties of the PEDOT-*g*-PCL copolymers increase as the PEDOT composition increases, whereas the printability properties will benefit from the PCL composition. For this reason, a balance

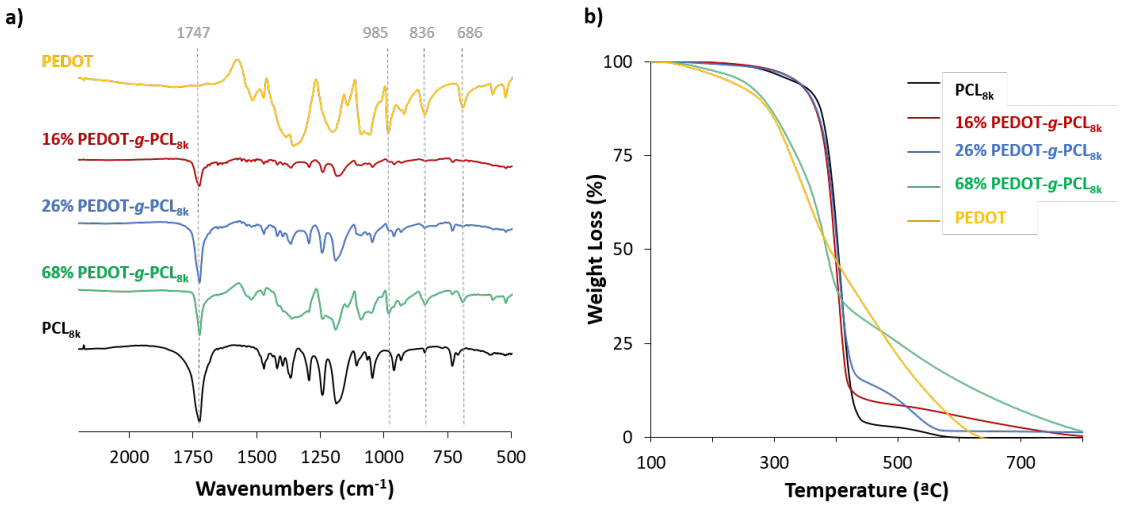

Figure 1. a) FT-IR and b) TGA spectra of the copolymers PEDOT-*g*-PCL_{8k} synthesized with different PEDOT compositions, 16, 26 and 68 %wt.

between both components of the graft copolymer needs to be found. Therefore, copolymers with different PEDOT percentages were synthesized by changing the initial EDOT:PCL ratio employed in the reaction. As can be observed in **Table 1**, higher yields (> 40%) are obtained when a low quantity of EDOT monomer is fed to the reaction (≤ 5%wt), as well as the molecular weight of the PCL macromonomer increases. The presence of both components, PCL and PEDOT, in the copolymers was monitored by infrared spectroscopy (**Figure 1a**). FT-IR spectra show the signals of the carbonyl group of PCL at 1747 cm^{-1} and the thiophene ring of PEDOT located at 985, 836 and 686 cm^{-1}. Besides, the presence of PEDOT in the copolymers was also confirmed by UV-vis-NIR spectroscopy. All spectra show the polaron and bipolaron absorption bands in the range 800 – 1000 nm (**Figure S2**, Supporting Information), which is characteristic of the PEDOT oxidized polymer.[31] Regarding the PEDOT composition in the PEDOT-*g*-PCL copolymers, it was calculated by TGA using the relative thermal stability of the copolymers at 450 °C (**Figure 1b**). As can be observed, all spectra present a proportional weight loss related to the PEDOT percentage in the copolymers. By comparing these results with the calibration curve obtained for different PEDOT/PCL blends (**Figure S3**, Supporting Information), it is possible to determine the percentage of PEDOT present in the synthesized copolymers PEDOT-*g*-PCL, and results are collected in Table 1. The PEDOT composition in the copolymers was much higher than the one fed to the reaction, and as expected, the final percentage of PEDOT in the copolymers increased with the initial EDOT percentage used in the feed. These results are in agreement with previous works for the synthesis of other graft copolymers such as PEDOT-*g*-PLA and PPy-*g*-PCL and associated with the low reactivity of the macronomers.[18, 26, 32] It was also observed an increase in the percentage of PEDOT incorporated in the copolymers as the molecular weight (M_n) of the PCL macromonomer decreased. This can be explained by the fact that more EDOT-end PCL chains are available to react with the EDOT monomer leading to PEDOT-*g*-PCL copolymers with a higher PEDOT percentage.

To evaluate the impact of the PEDOT presence in the copolymers to obtain homogeneous materials for additive manufacturing applications, the morphological structure was analysed by SEM (**Figure 2**). The PCL macromonomer shows a continuous morphology that is substantially affected by the incorporation of PEDOT within the copolymer chain PEDOT-*g*-PCL. As long as PEDOT is incorporated in the graft copolymer, the film morphology shows the presence of particles throughout the whole surface, whose density considerably increases with the PEDOT percentage. In the case of the copolymers with the highest PEDOT percentage, 68% PEDOT-*g*-PCL, the morphology is granular, almost similar to the one of neat PEDOT, which could hinder the

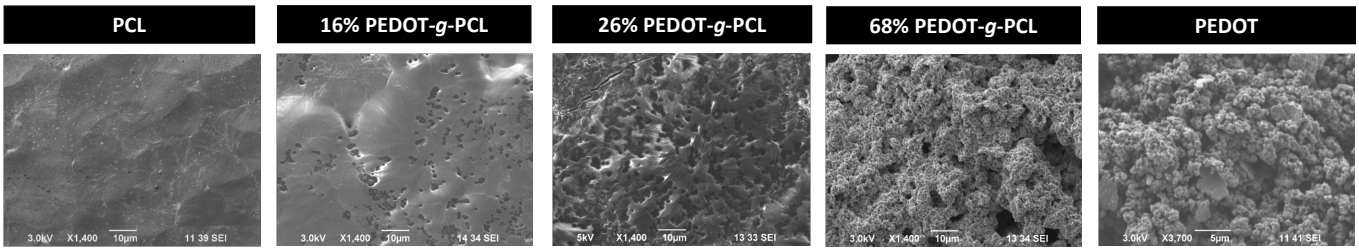

Figure 2. SEM images of films obtained by drop casting of PCL, PEDOT and different PEDOT-*g*-PCL_{8K} copolymer solutions in $CHCl_3$.

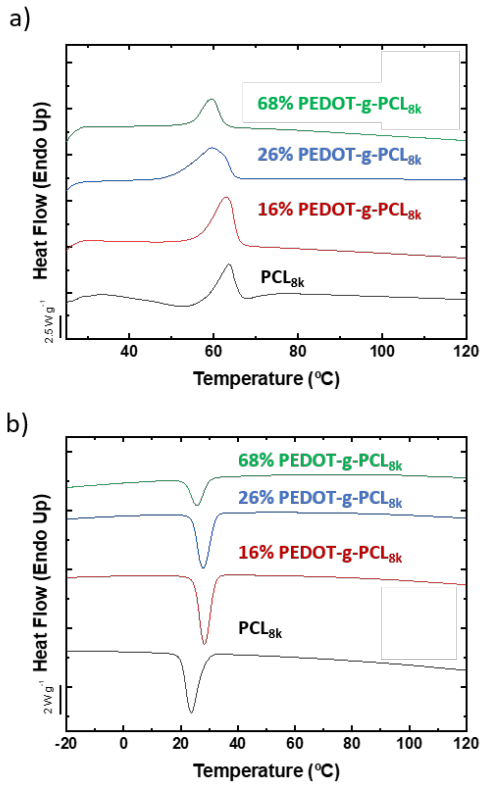

Figure 3. DSC spectra of PCL_{8k} and PEDOT-*g*-PCL_{8k} copolymers, a) 2nd heat scan at a temperature rate of 20 °C min^{-1} rate and b) cooling down scan at 20 °C min^{-1}.

the crystallization process from the melt. In that case, a shift to higher crystallization temperatures (T_c) is observed as long as PEDOT is incorporated in the copolymer, from T_c = 23°C for PCL up to 27°C and 29°C for 16% PEDOT-*g*-PCL and 68% PEDOT-*g*-PCL, respectively. Similar behaviour was observed for the copolymers PEDOT-*g*-PCL_{16k}, synthesized with higher M_n of the PCL macromonomer (**Figure S4**, Supporting Information). The increase in crystallization temperature of the PCL component is probably due to a nucleation effect, which could be caused by PEDOT incorporation.

The effect of the thermal treatment on the nanoscale morphology of the PEDOT-*g*-PCL copolymers was examined by AFM. For such purpose, the copolymers were solubilized in chloroform, drop casted on a silicon substrate, and subjected to the thermal protocol specified in the experimental section. AFM height images (**Figure 4**) show the characteristic lamellar structure of the PCL. In the case of PEDOT-*g*-PCL copolymers, this lamellar structure is altered by round-shape areas that increase the average roughness (R_a) from 5 nm for PCL to 12 nm for 26% PEDOT-*g*-PCL, due to the presence of PEDOT as observed by SEM. After the thermal treatment, the bigger size lamellae remained unaltered, but some small darker areas appear in the extrusion printing process. Even if the incorporation of PEDOT interrupts the flatten PCL morphology, each copolymer shows a homogeneous morphology from flat to rough particle surfaces for lower and higher PEDOT compositions respectively.

Prior to proceed with the additive manufacturing of these copolymers by direct ink writing in the melt state, the thermal properties need to be studied. DSC analysis was performed to evaluate the melting and crystallization processes of the graft copolymers under standard conditions. First, the sample was heated from room temperature up to 120°C at a rate of 20°C min^{-1} and then it was cooled down until -20°C at the same rate. **Figure 3a** exhibits the second DSC heating scans of PEDOT-*g*-PCL_{8k} copolymers. A single endothermic peak is observed above 53°C corresponding to the melting temperature (T_m) of the polyester (PCL). This melting temperature remains constant in the case of the copolymer with the highest PCL content, 16% PEDOT-*g*-PCL, while a shift to lower T_m is observed as the PEDOT percentage increases in the copolymers, T_m = 51°C for 26% PEDOT-*g*-PCL and T_m = 50°C for 68% PEDOT-*g*-PCL. As PEDOT is incorporated in the graft copolymer, the crystallisable linear PCL sequences are increasingly interrupted by the grafted chains, and thinner crystals are formed that melt at progressively lower temperatures. **Figure 3b** shows the DSC cooling down scan with the presence of a single exothermic peak, which is attributed to

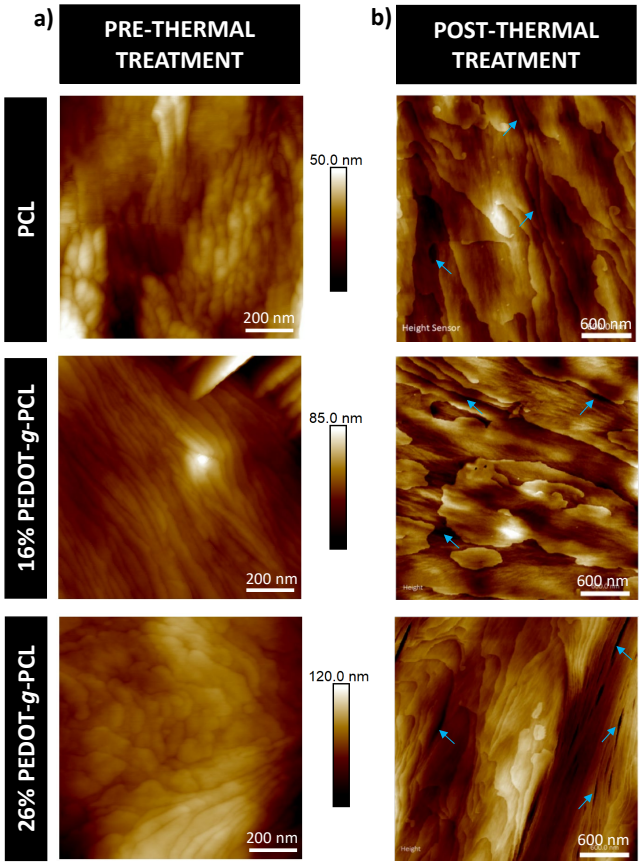

Figure 4. AFM images of films obtained by drop casting of PCL and different PEDOT-*g*-PCL_{8K} copolymer solutions in $CHCl_3$ pre- (a) and after- thermal treatment (b). Blue arrows highlight darker regions (lower height) after thermal treatment.

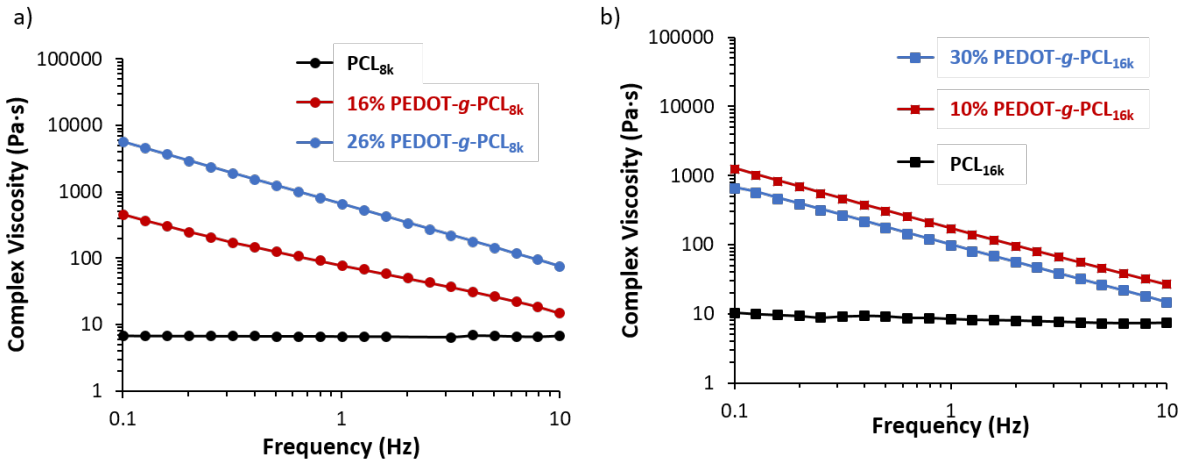

Figure 3. Complex viscosity at 65 °C of a) PCL_{8k} and PEDOT-*g*-PCL_{8k} copolymers, and b) PCL_{16k} and PEDOT-*g*-PCL_{16k} copolymers.

interlamellar regions. These darker areas are attributed to the presence of amorphous PCL regions. During the thermal treatment, the samples are heated to temperatures above the melting point of the PCL phase, then they are cooled to room temperature only. During cooling just to room temperature (see Figure 3b), it is possible that not all the previous thinner lamellae (that usually crystallize at lower temperatures) could be formed and the material where they were previously located is now constituting the amorphous interlamellar regions between the thickest lamellae (that formed at temperatures above 25 °C during cooling from the melt). A similar behaviour has also been observed for PCL-*co*-PLA diblock copolymers.[33] These results allow us to conclude that the main structure and morphology of the PEDOT-*g*-PCL copolymers is not substantially affected by the heating process over the melting point (as they are able to reform as expected), which makes them ideal candidates to be manufactured by DIW in the melt state.

3D printing of PEDOT-*g*-PCL copolymers

The additive manufacturing of PEDOT-*g*-PCL copolymers by 3D printing depends on their shear-thinning behaviour and ability to flow. Previously, we have reported that complex viscosities (η*) lower than 10^3 Pa·s represent the most liquid-like compositions to be processed by 3D extrusion printing, whereas higher than 10^4 Pa·s are characteristic of a solid-like behaviour. Complex viscosities between 10^3 Pa·s < η* < 10^4 Pa·s are indicative of solid to liquid transition with a high plasticity behaviour that hinders the polymer flow through the needle.[18] For such purpose, frequency sweeps were performed at the melting temperature of the polyester, *i.e.,* 65°C, (**Figure 5** and **S5**, Supporting information). In the case of the PCL macromonomer, a fluid-like behaviour is

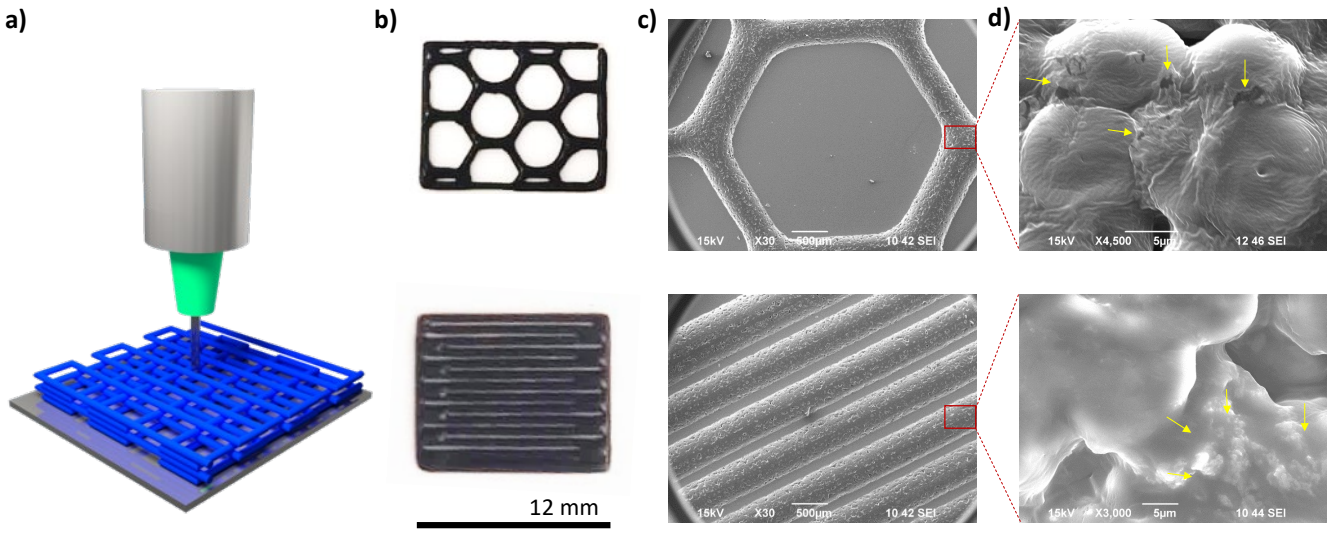

Figure 4. a) Schematic representation of the printing process. b) Pictures of the printed PEDOT-*g*-PCL patterns. Scale bar = 12 mm. c) Topographical SEM images of the printed patterns corresponding to 16% PEDOT-*g*-PCL_{8k} copolymers (top) and 26% PEDOT-*g*-PCL_{8k} copolymers (bottom). d) Zoom-in of the SEM pictures, where PEDOT particles are highlighted with yellow arrows.

observed with complex viscosity values lower than 10 Pa·s. The incorporation of PEDOT in the polymer chain gives rise to a huge increase in the complex viscosity reaching values of 400 and 5000 Pa·s for 16% PEDOT-*g*-PCL_{8k} and 26% PEDOT-*g*-PCL_{8k}, respectively. This latter case is ranged in the transition-like area and could present limitations to flow. It was also observed a decrease of the complex viscosity in the copolymers when the molecular weight of the PCL macromonomer (M_n) increases, reaching a value of $\eta^* = 600$ Pa·s for 30% PEDOT-*g*-PCL_{16k}. Nevertheless, all copolymers show a shear thinning behaviour with a high decrease of the complex viscosity with the frequency, which makes them accurate for 3D direct ink writing. Then, 3D printing tests were performed by DIW of these copolymers in the melting state (**Figure 6a**). In the case of the PCL macromonomers, they can be easily printed at the melting temperature (65°C) with minimal pressure. However, the copolymers PEDOT-*g*-PCL require the combination of both properties, melting state and a physical pressure, to be printed. Besides, the copolymers with complex viscosity values in the solid to liquid transition zone, 10^3 Pa·s < η^* < 10^4 Pa·s, present high plasticity, being necessary to combine the pneumatic pressure input by air with the mechanical action of a metallic piston to print them. Therefore, the copolymers PEDOT-*g*-PCL were inserted in a metallic extruder, warmed up at 65°C, and subsequently printed by air/physical action. The material was deposited layer-by-layer, forming three-dimensional structures.

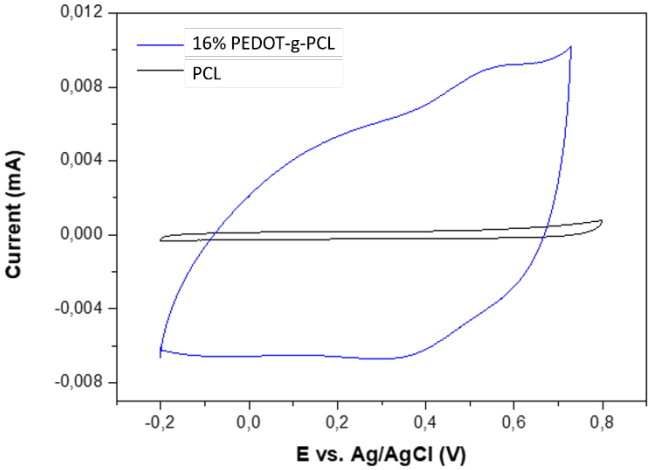

Figure 7. Comparison of the cyclic voltammograms of 16% PEDOT-*g*-PCL and PCL polymers in 0.1 M NaCl aqueous solution at 50 mV/s.

The PCL macromonomer and all the copolymers with PEDOT percentages between 10 and 30 %wt were successfully printed in a wide variety of complex shapes (**Figure 6b** and **S6**, Supporting Information). The structural characterization by SEM shows a very high resolution of the printed structures retaining their shape after printing (**Figure 6c** and **S6**, Supporting Information). It is worth mentioning that all the copolymers with PEDOT percentages between 10 and 30 %wt were successfully printed using the air/physical action. Then, the morphology of the printed copolymers was analysed in detail by zoom-in the printed area (**Figure 6d**). Some particles can be distinguished all around the material, as marked by yellow arrows, and their density increases with the PEDOT percentage in the copolymers, accordingly with the results obtained for the drop casted films.

Electrical properties of the 3D printed scaffolds

The conductivity of the printed scaffolds was measured with a four-point probe. In the case of the copolymers PEDOT-*g*-PCL_{8k}, there is an increase of the conductivity with the PEDOT percentage in the copolymers, from 1.17×10^{-4} S cm^{-1} for 16% PEDOT-*g*-PCL_{8k} to 7.07×10^{-4} S cm^{-1} for 26% PEDOT-*g*-PCL_{8k}. However, in the case of PEDOT-*g*-PCL_{16k} copolymers, synthesized with the PCL macromonomer of high molecular weight, the conductivity substantially decreases up to values of 3.10×10^{-5} S cm^{-1} and 4.26×10^{-5} S cm^{-1} for 10 and 30% PEDOT-*g*-PCL_{16k}, respectively. This conductivity is lower than the one obtained for highly conductive PEDOT:PSS; however, these values are in the same order as those obtained for other conducting graft copolymers such as PPy-*b*-PCL copolymers (2.8×10^{-4} S cm^{-1})[24] and PCL/PANI blends (2.5×10^{-4} S cm^{-1})[23], and higher than PCL/MWCNTs scaffolds (1.4×10^{-5} S cm^{-1})[34]. Taking into account that the conductive properties decrease for the copolymers with higher M_n of the PCL macromonomer, the copolymer 16% PEDOT-*g*-PCL_{8k} was chosen for further studies with 8220 muscle cells.

Electrochemical characterization was performed using cyclic voltammetry in 0.1 M NaCl aqueous solution. As can be observed in **Figure 7**, the cyclic voltammogram (CV) of 16% PEDOT-*g*-PCL shows a capacitive behavior and broad anodic and cathodic peaks at 0.55 V and 0.4 V vs Ag/AgCl, which are typical of PEDOT and demonstrates the electroactive behavior of the polymer. On the contrary, the CV of PCL is completely flat, indicating that is not electrochemically active. Besides, cyclic voltammetries at different scan rates were performed to analyze charge transfer processes. The CV at various scan rates of a 16% PEDOT-*g*-PCL film in 0.1 M NaCl aqueous solution are shown in **Figure S7**. The anodic and cathodic currents increase proportionally with the scan rate, indicating that the redox process is not limited by diffusion, and demonstrating that the whole PEDOT-*g*-PCL film is involved in the electrochemical reaction.

Muscle cells culture onto PCL and electroactive PEDOT-*g*-PCL patterns

As mentioned before, muscle tissues are formed by a skeletal muscle fiber arrangement of myotubes unidirectionally aligned.[6] To that aim, patterns with different distances between strands, 460 µm for large width and 230 µm for small width, were printed to induce the muscle cells alignment (**Figure 8a**). Firstly, the biocompatibility of these printed scaffolds was assessed. For such purpose, 8220 muscle cells were cultured on the printed scaffolds, and cell toxicity after 24 hours culture was calculated by a direct lactate dehydrogenase (LHD) assay measuring the absorbance at 490 nm (**Figure 8b**). As can be observed, there are not significant differences in the absorbance for the PCL and PEDOT-*g*-PCL scaffolds as comparing with the gelatin-coated plate used as control

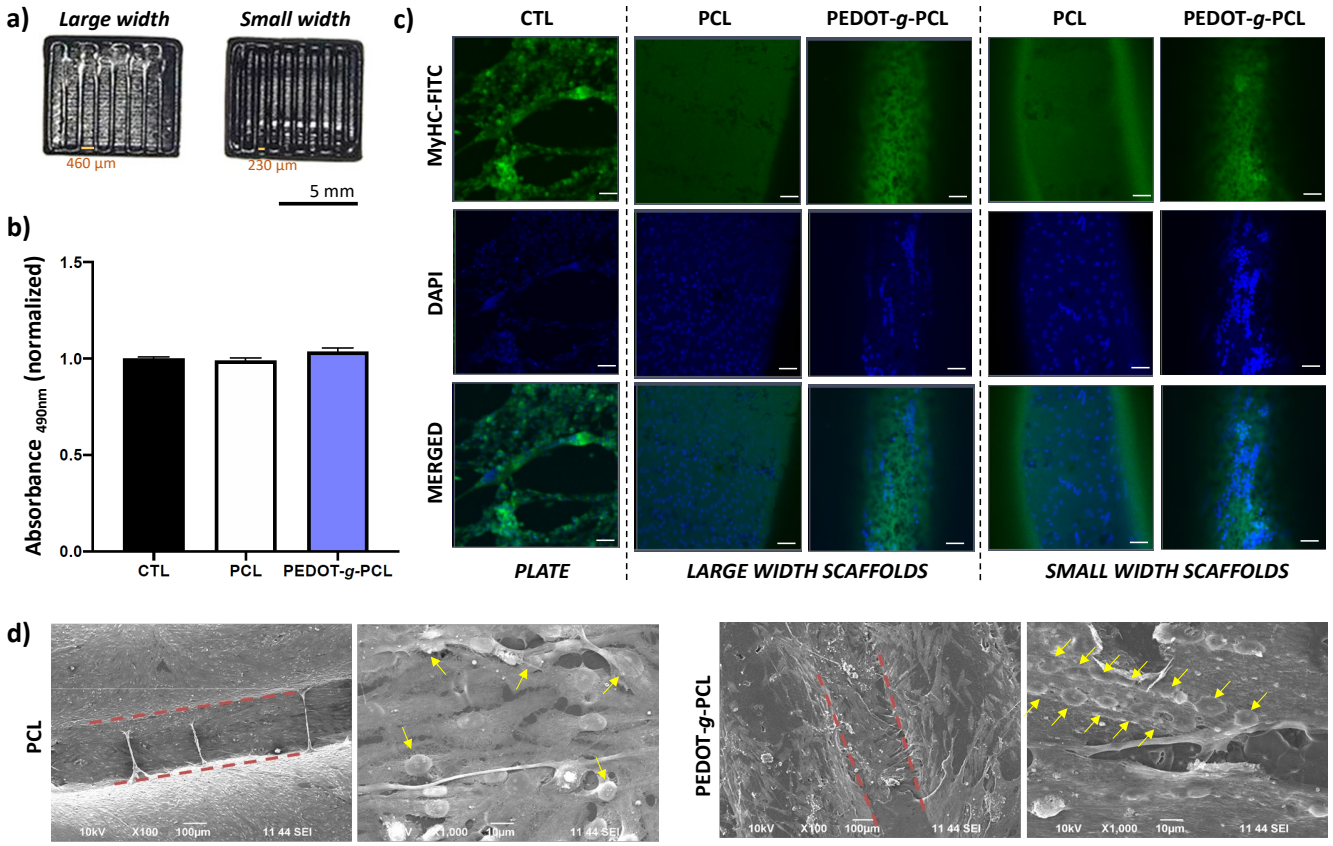

Figure 8. a) Printed patterns employed for cellular tests. Large width patterns possess 460 µm width between strands and small width patterns 230 µm. b) LDH test to determine the 8220 muscle cell toxicity after 24 h. Non-significant differences with $^{**}p \leq 0.05$. c) Immunofluorescence images of 8220 muscle cells after 5 days culture on the plate (CTL) and on PCL or PEDOT-*g*-PCL scaffolds with large width and small width between strands. Cytoskeleton stained in green with MyHC-FITC (top), nuclei stained in blue with DAPI (center) and merged channels (bottom). Scale bar = 50 µm. d) SEM images of 8220 muscle cells cultured on PCL or PEDOT-*g*-PCL small width scaffolds, where channels are delimited by dashed red lines, and zoom-in of the channel area between strands where nuclei are highlighted with yellow arrows.

(CTL), which means that the cell viability is not altered in contact with the PCL and PEDOT-*g*-PCL scaffolds proving the non-cytotoxic behaviour of the materials. Then, the effect of the composition and design of the printed scaffolds on the myoblasts cell alignment and differentiation was studied by immunofluorescent staining using myosin heavy chain (MyHC), a myotube maturation marker (**Figure 8c**). A robust green fluorescence for MyHC is observed in the case of the patterns made with the copolymer PEDOT-*g*-PCL following the strand direction of the printed pattern. This is also corroborated by the blue fluorescence (DAPI) of the nuclei oriented along the channel between strands meaning that muscle cells are more fused tending to form myotubes. That is not observed in the case of the PCL scaffolds, where nuclei are randomly distributed all over the channel with not robust MyHC fluorescence intensity, meaning that myoblasts are not aligned. Cells are not either aligned in the case of CTL samples. This achievement was also corroborated by SEM characterization (**Figure 8d**). Cells adhere on the PCL and PEDOT-*g*-PCL scaffolds surface; however, in the case of PCL scaffolds, nuclei are randomly distributed, whereas on PEDOT-*g*-PCL scaffolds, nuclei are clearly aligned, as indicated by the yellow arrows. Alignment of muscle cells depends on cell confluence, material composition, patterning, surface energy and wettability. PEDOT-*g*-PCL patterns are more hydrophilic (WCA = 49 ± 7°) than PCL ones (WCA = 70 ± 3°), as shown in Figure S8, which could favour the cell adhesion, a primary step for the later cell proliferation and differentiation.[35] Apart from that, conductive materials can promote proliferation and differentiation when responsive cells are cultured on top or within them.[36-37] In that sense, we have shown by the four-point probe and CV experiments that PEDOT-*g*-PCL scaffolds are electroactive, whereas PCL scaffolds do not exhibit that property. It means that PEDOT-*g*-PCL scaffolds are able to provide electrical stimulation *per se* to the cells in contact with them favouring the chemical exchanges and signal communications among the cells at the interface of cell membrane-material inducing their alignment. Therefore, the combination of different specific properties exhibited by PEDOT-*g*-PCL materials, including chemical composition, conductivity, redox activity and hydrophilicity changes, ensures differences in cell alignment and myogenesis. Indeed, the presence of MyHC marker could be indicative of myotubes differentiation in the case of the PEDOT-*g*-PCL, corroborating the hypothesis. Therefore, this type of 3D printed conducting scaffolds could mimic native skeletal muscle architecture for potential tissue engineering applications.

Conclusions

PEDOT-*g*-PCL copolymers with different molecular weights and compositions, were synthesized by chemical oxidative polymerization of EDOT and α–EDOT-PCL macromonomers, which were previously synthesized by ring-opening polymerization of εCL initiated by EDOT-methanol. The copolymerization process reached yields higher than 40% in the case of copolymers with lower PEDOT composition, 10% PEDOT-*g*-$PCL_{16k,}$ and 16% PEDOT-*g*-PCL_{8k}. All the copolymers show a shear-thinning behaviour with a drastic decrease of the viscosity as the frequency increases. However, only the copolymers with lower PEDOT percentages show complex viscosity values lower than 10^3 Pa·s to be easily processed by direct ink writing. The copolymers were successfully printed by DIW in different shapes. It was also determined that the melting process did not produce significant changes in the global morphology of the material, and larger size lamellar were able to reformed during cooling after the thermal treatment. Moreover, SEM images showed high resolution images of these printed patterns with conductivity values of 1.17×10^{-4} S **c**m^{-1} for 16% PEDOT-*g*-PCL_{8k} and 7.07×10^{-4} S **c**m^{-1} for 26% PEDOT-*g*-PCL_{8k}, as determined by the four-point probe. Finally, the biocompatibility properties of the printed scaffolds were proven in contact with 8220 muscle cells, as well as their ability to induce the cell alignment and myotubes differentiation mimicking the native muscle tissue for tissue engineering applications. These polymers show promising properties as artificial three-dimensional scaffolds mimicking the native skeletal muscle architecture for potential applications in bioelectronics.

Conflicts of interest

There are no conflicts to declare.

Acknowledgements

This work was funded by the Spanish AEI-MICINN project PID2020-119026GB-I00 and Basque Government through grant IT1309-19. J.L.O.-M. thanks the Consejo Nacional de Ciencia y Tecnología (CONACyT, México) for the grant awarded no. 471837.

References

(1) Alegret, N.; Dominguez-Alfaro, A.; Mecerreyes, D., Chapter 10 Conductive Polymers Building 3D Scaffolds for Tissue Engineering. In *Redox Polymers for Energy and Nanomedicine*, The Royal Society of Chemistry: **2021**, pp 383-414.

(2) Yang, J. C.; Mun, J.; Kwon, S. Y.; Park, S.; Bao, Z.; Park, S., Electronic Skin: Recent Progress and Future Prospects for Skin-Attachable Devices for Health Monitoring, Robotics, and Prosthetics. *Adv. Mater.* **2019,** *31* (48), 1904765.

(3) Maziz, A.; Özgür, E.; Bergaud, C.; Uzun, L., Progress in conducting polymers for biointerfacing and biorecognition applications. *Sens. Actuators Rep.* **2021,** *3*, 100035.

(4) Alegret, N.; Dominguez-Alfaro, A.; Mecerreyes, D., 3D Scaffolds Based on Conductive Polymers for Biomedical Applications. *Biomacromolecules* **2019,** *20* (1), 73-89.

(5) Qi, Z.; Ye, J.; Chen, W.; Biener, J.; Duoss, E. B.; Spadaccini, C. M.; Worsley, M. A.; Zhu, C., 3D-Printed, Superelastic Polypyrrole–Graphene Electrodes with Ultrahigh Areal Capacitance for Electrochemical Energy Storage. *Adv. Mater. Technol.* **2018,** *3* (7), 1800053.

(6) Zhao, Y.; Zeng, H.; Nam, J.; Agarwal, S., Fabrication of skeletal muscle constructs by topographic activation of cell alignment. *Biotechnol. Bioeng.* **2009,** *102* (2), 624-631.

(7) Kim, G.-W.; Nam, G.-H.; Kim, I.-S.; Park, S.-Y., Xk-related protein 8 regulates myoblast differentiation and survival. *FEBS J.* **2017,** *284* (21), 3575-3588.

(8) Ligon, S. C.; Liska, R.; Stampfl, J.; Gurr, M.; Mülhaupt, R., Polymers for 3D Printing and Customized Additive Manufacturing. *Chem. Rev.* **2017,** *117* (15), 10212-10290.

(9) Criado-Gonzalez, M.; Dominguez-Alfaro, A.; Lopez-Larrea, N.; Alegret, N.; Mecerreyes, D., Additive Manufacturing of Conducting Polymers: Recent Advances, Challenges, and Opportunities. *ACS Appl. Polym. Mater.* **2021,** *3* (6), 2865-2883.

(10) Narupai, B.; Nelson, A., 100th Anniversary of Macromolecular Science Viewpoint: Macromolecular Materials for Additive Manufacturing. *ACS Macro Lett.* **2020,** *9* (5), 627-638.

(11) Minudri, D.; Mantione, D.; Dominguez-Alfaro, A.; Moya, S.; Maza, E.; Bellacanzone, C.; Antognazza, M. R.; Mecerreyes, D., Water Soluble Cationic Poly(3,4-Ethylenedioxythiophene) PEDOT-N as a Versatile Conducting Polymer for Bioelectronics. *Adv. Electron. Mater.* **2020,** *6* (10), 2000510.

(12) Yuk, H.; Lu, B.; Lin, S.; Qu, K.; Xu, J.; Luo, J.; Zhao, X., 3D printing of conducting polymers. *Nat. Commun.* **2020,** *11* (1), 1604.

(13) Bao, P.; Lu, Y.; Tao, P.; Liu, B.; Li, J.; Cui, X., 3D printing PEDOT-CMC-based high areal capacity electrodes for Li-ion batteries. *Ionics* **2021,** *27* (7), 2857-2865.

(14) Françon, H.; Wang, Z.; Marais, A.; Mystek, K.; Piper, A.; Granberg, H.; Malti, A.; Gatenholm, P.; Larsson, P. A.; Wågberg, L., Ambient-Dried, 3D-Printable and Electrically Conducting Cellulose Nanofiber Aerogels by Inclusion of Functional Polymers. *Adv. Funct. Mater.* **2020,** *30* (12), 1909383.

(15) Spencer, A. R.; Shirzaei Sani, E.; Soucy, J. R.; Corbet, C. C.; Primbetova, A.; Koppes, R. A.; Annabi, N., Bioprinting of a Cell-Laden Conductive Hydrogel Composite. *ACS Appl. Mater. Interfaces* **2019,** *11* (34), 30518-30533.

(16) Manavitehrani, I.; Fathi, A.; Badr, H.; Daly, S.; Negahi Shirazi, A.; Dehghani, F., Biomedical Applications of Biodegradable Polyesters. *Polymers* **2016,** *8* (1), 20.

(17) Gonçalves, F. A. M. M.; Fonseca, A. C.; Domingos, M.; Gloria, A.; Serra, A. C.; Coelho, J. F. J., The potential of unsaturated polyesters in biomedicine and tissue engineering: Synthesis, structure-properties relationships and additive manufacturing. *Prog. Polym. Sci.* **2017,** *68*, 1-34.

(18) Dominguez-Alfaro, A.; Gabirondo, E.; Alegret, N.; De León-Almazán, C. M.; Hernandez, R.; Vallejo-Illarramendi, A.; Prato, M.; Mecerreyes, D., 3D Printable Conducting and Biocompatible PEDOT-graft-PLA Copolymers by Direct Ink Writing. *Macromol. Rapid Commun.* **2021,** *42* (12), 2100100.

(19) Fortelny, I.; Ujcic, A.; Fambri, L.; Slouf, M., Phase Structure, Compatibility, and Toughness of PLA/PCL Blends: A Review. *Front. Mater.* **2019,** *6* (206).

(20) Zhang, C.; Lan, Q.; Zhai, T.; Nie, S.; Luo, J.; Yan, W., Melt Crystallization Behavior and Crystalline Morphology of Polylactide/Poly(ε-caprolactone) Blends Compatibilized by Lactide-Caprolactone Copolymer. *Polymers* **2018,** *10* (11), 1181.

(21) Fenni, S. E.; Cavallo, D.; Müller, A. J., Nucleation and Crystallization in Bio-Based Immiscible Polyester Blends. In *Thermal Properties of Bio-based Polymers*, Di Lorenzo, M. L.; Androsch, R., Eds. Springer International Publishing: Cham, **2019**, pp 219-256.

(22) Ritzau-Reid, K. I.; Spicer, C. D.; Gelmi, A.; Grigsby, C. L.; Ponder Jr, J. F.; Bemmer, V.; Creamer, A.; Vilar, R.; Serio, A.; Stevens, M. M., An Electroactive Oligo-EDOT Platform for Neural Tissue Engineering. *Adv. Funct. Mater.* **2020,** *30* (42), 2003710.

(23) Wibowo, A.; Vyas, C.; Cooper, G.; Qulub, F.; Suratman, R.; Mahyuddin, A. I.; Dirgantara, T.; Bartolo, P., 3D Printing of Polycaprolactone–Polyaniline Electroactive Scaffolds for Bone Tissue Engineering. *Materials* **2020,** *13* (3), 512.

(24) Vijayavenkataraman, S.; Kannan, S.; Cao, T.; Fuh, J. Y. H.; Sriram, G.; Lu, W. F., 3D-Printed PCL/PPy Conductive Scaffolds as Three-Dimensional Porous Nerve Guide Conduits (NGCs) for Peripheral Nerve Injury Repair. *Front. Bioeng. Biotechnol.* **2019,** *7* (266).

(25) Bendrea, A.-D.; Cianga, L.; Ailiesei, G.-L.; Ursu, E.-L.; Göen Colak, D.; Cianga, I., 3,4-Ethylenedioxythiophene (EDOT) End-Group Functionalized Poly-ε-caprolactone (PCL): Self-Assembly in Organic Solvents and Its Coincidentally Observed Peculiar Behavior in Thin Film and Protonated Media. *Polymers* **2021,** *13* (16), 2720.

(26) Mecerreyes, D.; Stevens, R.; Nguyen, C.; Pomposo, J. A.; Bengoetxea, M.; Grande, H., Synthesis and characterization of polypyrrole-graft-poly(ε-caprolactone) copolymers: new electrically conductive nanocomposites. *Synth. Met.* **2002,** *126* (2), 173-178.

(27) da Silva, A. C.; Augusto, T.; Andrade, L. H.; Córdoba de Torresi, S. I., One pot biocatalytic synthesis of a biodegradable electroactive macromonomer based on 3,4-ethylenedioxytiophene and poly(l-lactic acid). *Mater. Sci. Eng., C* **2018,** *83*, 35-43.

(28) da Silva, A. C.; Semeano, A. T. S.; Dourado, A. H. B.; Ulrich, H.; Cordoba de Torresi, S. I., Novel Conducting and Biodegradable Copolymers with Noncytotoxic Properties toward Embryonic Stem Cells. *ACS Omega* **2018,** *3* (5), 5593-5604.

(29) Molina, B. G.; Bendrea, A. D.; Cianga, L.; Armelin, E.; del Valle, L. J.; Cianga, I.; Alemán, C., The biocompatible polythiophene-g-polycaprolactone copolymer as an efficient dopamine sensor platform. *Polym. Chem.* **2017,** *8* (39), 6112-6122.

(30) Basterretxea, A.; Gabirondo, E.; Jehanno, C.; Zhu, H.; Coulembier, O.; Mecerreyes, D.; Sardon, H., Stereoretention in the Bulk ROP of l-Lactide Guided by a Thermally Stable Organocatalyst. *Macromolecules* **2021,** *54* (13), 6214-6225.

(31) Luo, J.; Billep, D.; Waechtler, T.; Otto, T.; Toader, M.; Gordan, O.; Sheremet, E.; Martin, J.; Hietschold, M.; Zahn, D. R. T.; Gessner, T., Enhancement of the thermoelectric properties of PEDOT:PSS thin films by post-treatment. *J. Mater. Chem. A* **2013,** *1* (26), 7576-7583.

(32) Marina, S.; Mantione, D.; ManojKumar, K.; Kari, V.; Gutierrez, J.; Tercjak, A.; Sanchez-Sanchez, A.; Mecerreyes, D., New electroactive macromonomers and multi-responsive PEDOT graft copolymers. *Polym. Chem.* **2018,** *9* (27), 3780-3790.

(33) Palacios, J. K.; Zhang, H.; Zhang, B.; Hadjichristidis, N.; Müller, A. J., Direct identification of three crystalline phases in PEO-b-PCL-b-PLLA triblock terpolymer by In situ hot-stage atomic force microscopy. *Polymer* **2020,** *205*, 122863.

(34) e Silva, E. P.; Huang, B.; Helaehil, J. V.; Nalesso, P. R. L.; Bagne, L.; de Oliveira, M. A.; Albiazetti, G. C. C.; Aldalbahi, A.; El-Newehy, M.; Santamaria-Jr, M.; Mendonça, F. A. S.; Bártolo, P.; Caetano, G. F., In vivo study of conductive 3D printed PCL/MWCNTs scaffolds with electrical stimulation for bone tissue engineering. *Bio-Des. Manuf.* **2021,** *4* (2), 190-202.

(35) Wan, Y.; Qu, X.; Lu, J.; Zhu, C.; Wan, L.; Yang, J.; Bei, J.; Wang, S., Characterization of surface property of poly(lactide-co-glycolide) after oxygen plasma treatment. *Biomaterials* **2004,** *25* (19), 4777-4783.

(36) Wang, S.; Sun, C.; Guan, S.; Li, W.; Xu, J.; Ge, D.; Zhuang, M.; Liu, T.; Ma, X., Chitosan/gelatin porous scaffolds assembled with conductive poly(3,4-ethylenedioxythiophene) nanoparticles for neural tissue engineering. *J. Mater. Chem. B* **2017,** *5* (24), 4774-4788.

(37) Guex, A. G.; Puetzer, J. L.; Armgarth, A.; Littmann, E.; Stavrinidou, E.; Giannelis, E. P.; Malliaras, G. G.; Stevens, M. M., Highly porous scaffolds of PEDOT:PSS for bone tissue engineering. *Acta Biomater.* **2017,** *62*, 91-101.